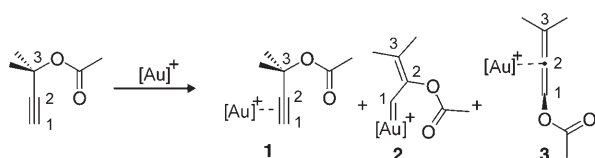


## Reaction Mechanisms

## Golden Carousel in Catalysis: The Cationic Gold/Propargylic Ester Cycle\*\*

Andrea Correa, Nicolas Marion, Louis Fensterbank, Max Malacria, Steven P. Nolan, and Luigi Cavallo\*

Gold-mediated homogeneous catalysis is rapidly growing in popularity, with a variety of applications described in recent reviews.<sup>[1]</sup> Alkynes are among the most versatile substrates, and the potential of easily accessible propargylic esters is currently being investigated by several groups.<sup>[2]</sup> However, this chemistry is still in its infancy, and results are often surprising and in some cases difficult to explain. It is known that under Au catalysis, gold propargylic esters species such as **1** undergo 1,2- and 1,3-acyl migration,<sup>[3–6]</sup> leading to the formation of gold vinyl carbenoid species such as **2** and gold allene species such as **3** (Scheme 1). Of course, the Au-

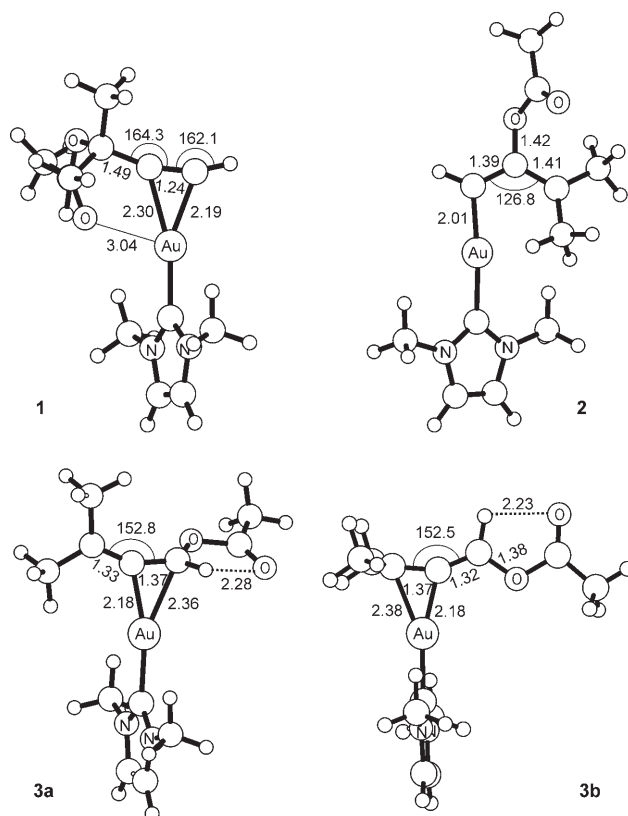


Scheme 1. Key intermediates along the catalytic cycle.

activated species **1–3** are the starting points for further reactions, leading to a great diversity of products.<sup>[7]</sup> Unfortunately, the thermodynamics and the sequence of reactions connecting the three key intermediates are not yet clear, and theoretical studies related to this topic are scarce.<sup>[4e,8–9]</sup> In this communication we propose, on the basis of DFT calculations,

that the three species can interconvert easily, forming a “golden carousel”. Specifically, we focused on cationic Au<sup>I</sup>L catalytic systems with L = PMe<sub>3</sub> and 2,3-dimethylimidazol-2-ylidene (IME), that is, the basic skeletons of phosphines and N-heterocyclic carbene (NHC) ligands, the latter of which have emerged as alternatives to phosphines.<sup>[10–12]</sup> We first briefly discuss the structural features of the three key intermediates in the case of L = NHC and then describe the reaction pathways interconnecting these intermediates with both L = PMe<sub>3</sub> and IME. All results are based on DFT calculations and include solvent effects.

The structures of the key intermediates **1–3** in the case of L = IME are depicted in Figure 1. The propargylic ester is slightly asymmetrically coordinated to the Au center in **1**, with the terminal alkynyl C1 atom closer to the metal. The C–C triple bond is only 0.03 Å longer than in the free ester, while the substituents on the C–C triple bond deviate from linearity

Figure 1. Structures of the [(IME)Au]-coordinated propargylic ester **1**, the gold vinyl carbenoid species **2**, and the gold allene type species **3a** and **3b**. Distances in Å.

[\*] Dr. A. Correa, Prof. Dr. L. Cavallo  
Department of Chemistry  
University of Salerno  
Ponte don Melillo, 84084 Fisciano (Italy)  
Fax: (+39) 089-969-603  
E-mail: lcavallo@unisa.it  
Homepage: <http://www.molnac.unisa.it/>

N. Marion, Prof. Dr. S. P. Nolan  
Institute of Chemical Research of Catalonia (ICIQ)  
Av. Països Catalans 16, 43007 Tarragona (Spain)  
Prof. Dr. L. Fensterbank, Prof. Dr. M. Malacria  
Université Pierre et Marie Curie—Paris 6  
Laboratoire de Chimie Organique  
UMR 7611 - FR 2769 B.229  
4 place Jussieu, 75005 Paris (France)

[\*\*] L.C. thanks the Regione Campania (Progetto Legge 5, 2006) for financial support, and CINECA (INSTM grant) for computer time. S.P.N. acknowledges the Petroleum Research Fund administered by the ACS, the Ministerio de Educación y Ciencia, the ICIQ Foundation and ICREA for partial funding. S.P.N. is an ICREA Research Professor. N.M. thanks the AGAUR for a pre-doctoral fellowship (2007 FI\_A01466). L.F. and M.M. thank the ANR “allènes” BLAN 06-2\_159258.

by roughly  $15^\circ$  only. The gold vinyl carbenoid **2** is characterized by almost equally long C1–C2 and C2–C3 bonds.<sup>[13]</sup> This suggests that the positive charge is highly delocalized in  $\pi$  orbitals of the conjugated system involving the Au, C1, C2, C3, and O atoms. Finally, in the gold allene species the Au is coordinated to either the C1–C2 or C2–C3 double bond (structures **3a** and **3b**, respectively, in Figure 1). In both structures the coordinated double bond is only 0.04–0.05 Å longer than the uncoordinated double bond, and the C1–C2–C3 allene skeleton deviates roughly  $25^\circ$  from linearity. Calculations indicated that the two structures are at the same energy for L = IMe, with **3b** only 0.1 kcal mol<sup>-1</sup> lower in energy than **3a**, while for L = PMe<sub>3</sub> this preference for **3b** is slightly higher, 0.6 kcal mol<sup>-1</sup>. After this brief structural characterization, we now consider how these key intermediates interconvert in a merry-go-round fashion.

**1,2-shifts.** The *5-exo-dig* attack of the carboxylic O atom of **1** to the C2 atom of the alkynyl group leads to the five-membered cyclic intermediate **1-2**, which presents a single Au–C  $\sigma$  bond (see Figure 2). With L = IMe this cyclization step presents a rather low barrier, only 2.4 kcal mol<sup>-1</sup> (Figure 2), while replacing the IMe ligand with PMe<sub>3</sub> lowers this cyclization barrier to 0.7 kcal mol<sup>-1</sup> only. No ligand effect is detected for the reverse ring-opening step, which presents a very similar barrier for both systems, about 9 kcal mol<sup>-1</sup>.<sup>[14]</sup>

For L = IMe, intermediate **1-2** is 5.9 kcal mol<sup>-1</sup> more stable than the starting structure **1**, and can further evolve, through a ring-opening reaction, into the gold vinyl carbenoid

intermediate **2**, which is 0.4 kcal mol<sup>-1</sup> less stable than the starting Au-coordinated ester **1**. This ring-opening step presents a barrier of 9.4 kcal mol<sup>-1</sup>, while the reverse *5-exo-trig* reaction is very facile, with a barrier of only 3.1 kcal mol<sup>-1</sup>. Replacing the NHC ligand with PMe<sub>3</sub> improves the stability of **1-2** and particularly of **2**, which are 8.6 and 1.1 kcal mol<sup>-1</sup> more stable than **1**. The ring opening and the reverse *5-exo-trig* steps that connect **1-2** and **2** present barriers comparable to those calculated with the NHC ligand. The overall skeletal rearrangement **1**→**2** corresponds to the 1,2-shift of the carboxylic group from the propargylic position to the internal C2 atom of the alkynyl group.

The *5-exo-trig* attack of the carboxylic O atom of **2** at the C1 atom leads to the five-membered cyclic intermediate **2-3**. This cyclization step has also a rather low barrier, around 4 kcal mol<sup>-1</sup>, for both L = IMe and PMe<sub>3</sub>. The reverse ring-opening step requires crossing a higher energetic barrier for both systems, 8.6 and 10.0 kcal mol<sup>-1</sup> for L = IMe and PMe<sub>3</sub>, respectively. Intermediate **2-3** is more stable than **1** by 4.1 and 6.7 kcal mol<sup>-1</sup> with the IMe and PMe<sub>3</sub> ligands, respectively.

The Au shift toward the nearby C2(sp<sup>2</sup>) atom causes the ring opening of **2-3** and leads to the formation of the gold allene species **3a**, which is in rapid equilibrium with the slightly more stable species **3b** (by 0.1 and 0.6 kcal mol<sup>-1</sup> with IMe and PMe<sub>3</sub>, respectively). Intermediates **3a** and **3b** are 8 kcal mol<sup>-1</sup> more stable than intermediate **1** for L = IMe, and roughly 9 kcal mol<sup>-1</sup> more stable for L = PMe<sub>3</sub>. In the case of the IMe ligand, ring-opening of **2-3** to yield **3** costs 10.4 kcal mol<sup>-1</sup>, while the reverse *5-exo-dig* step presents the slightly higher barrier of 14.4 kcal mol<sup>-1</sup>. Replacing the NHC ligand with PMe<sub>3</sub> has no substantial effect on the barriers between **2-3** and **3**. As in the case of the **1**→**2** rearrangement, the **2**→**3** skeletal rearrangement corresponds to a 1,2-shift of the carboxylic group. With the model NHC and PR<sub>3</sub> ligands, and with the basic propargylic ester considered, the double 1,2-shift sequence is an energetically downhill path from the Au-coordinated propargylic ester **1** to the substantially isoenergetic gold vinyl carbenoid species **2**, and finally to the most stable gold allene species **3**.

**1,3-shift.** However, the gold allene **3** can be reached from the Au-coordinated propargylic ester **1** through a shorter reaction pathway. Indeed, *6-endo-dig* attack of the carboxylic O atom of **1** to the C1 atom of the alkynyl group leads to the six-membered cyclic intermediate **1-3**. This cyclization step is characterized by an energy barrier of 8.5 kcal mol<sup>-1</sup> for L = IMe, and it is roughly 2 kcal mol<sup>-1</sup> lower for L = PMe<sub>3</sub>. The reverse ring-opening step presents the highest barrier we calculated, about 15–16 kcal mol<sup>-1</sup> for both systems, which nevertheless remains a modest energy barrier. Intermediate **1-3** is more stable than **1** by 6.9 and 9.3 kcal mol<sup>-1</sup> for L = IMe and PMe<sub>3</sub>, respectively.

Intermediate **1-3** can further evolve, through a ring-opening step, into the gold allene species **3**, with the very low barrier of about 3 kcal mol<sup>-1</sup> with both the NHC and PMe<sub>3</sub> ligands. The reverse *6-endo-trig* reaction is energetically easily accessible as well, with a barrier of some 3 kcal mol<sup>-1</sup> for both L = IMe and PMe<sub>3</sub>. The overall

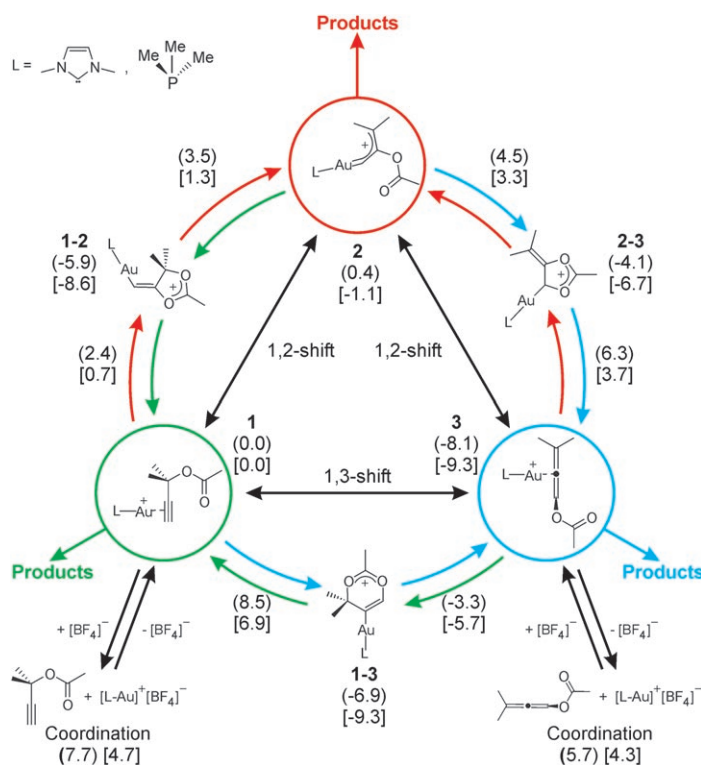


**Figure 2.** Schematic representation of the thermodynamics associated with the  $1 \rightleftharpoons 2 \rightleftharpoons 3 \rightleftharpoons 1$  equilibrium. Energies in kcal mol<sup>-1</sup> (in round/square brackets for L = IMe and PMe<sub>3</sub>, respectively) are calculated relative to **1**. Numbers close to the arrows represent the energy of the transition state associated with that reaction step.

skeletal rearrangement **1**→**3** corresponds to the 1,3-shift of the carboxylic group from the propargylic position to the terminal C atom of the alkynyl group.

*1,2- vs. 1,3-shift.* Comparison of the reaction pathways corresponding to a double 1,2-shift and to a direct 1,3-shift suggests that the double 1,2-shift is preferred for both systems, since the highest energy transition state along this pathway (**2**→**3**) is lower in energy than the highest energy transition state along the pathway of the direct 1,3-shift (**1**→**1-3**). Nevertheless, the preference for the double 1,2-shift pathway (roughly 2–3 kcal mol<sup>-1</sup>) is not particularly strong, which indicates that different NHC or PR<sub>3</sub> ligands and/or substrates could influence this preference for the double 1,2-shift.<sup>[15]</sup> This could explain the experimentally observed preference for 1,2- or 1,3-shift as a function of structural features of the substrate.<sup>[3c,5a,9a,b,16]</sup>

Indeed, it is more correct to claim that the two reaction paths are competitive, and that the three key species **1**, **2**, and **3** are in rapid equilibrium, with interconversion running fast both clockwise and counterclockwise in the cycle of Figure 2.<sup>[17]</sup> The exact way off this merry-go-round depends on the energy barriers associated with reactions involving intermediates **1**, **2**, and **3** and leading to products irreversibly. Of course, the reactivity of these intermediates also depends on other functional groups (typically, C–C double bonds and heteronucleophiles) on the substrate, on the nature of the NHC or phosphine ligand, and on the reaction conditions as well.

A potentially relevant difference between the L = IMe and PMe<sub>3</sub> systems is related to the most stable intermediate in the cycle. In the case of L = IMe the most stable intermediate clearly is **3** while, considering the level of accuracy of this kind of calculations, around 1–2 kcal mol<sup>-1</sup>, in the case of L = PMe<sub>3</sub> intermediate **1-2** at the antipodes is comparable in energy to **3**. This could imply that in the case of NHC ligands, intermediate **3** acts as reservoir of active species and that it could be the preferential way to exit the cycle, with an allene-based reactivity. In contrast, for the phosphine case there is no preferential way out of the cycle. Indeed, it could be **3** as in the case of the NHCs, but it could also be the almost isoenergetic intermediates **1** and **2**, with their specific reactivity, which are easily accessible from the relatively stable **1-2** intermediate. Again, the nature of the L ligand and/or of the substrate can influence this conclusion.

This reaction pathway manifold explains the variety of products that can be achieved by this kind of catalysis. The results we have presented here indicate that understanding the mechanistic details and the effect of the different variables (substrate, Au ligand, solvent, etc.) is the challenge to be addressed in order to control this powerful catalysis, and to direct the outcome of the reaction toward the selective synthesis of a desired product. We are currently working in this direction, using a combined experimental and theoretical approach.

Finally, we remark that entry points into the catalytic cycle are coordination of propargylic ester to the [AuL]<sup>+</sup>[BF<sub>4</sub>]<sup>-</sup> species to displace the [BF<sub>4</sub>]<sup>-</sup> counterion to give **1**, with an energy gain of 7.7 and 4.7 kcal mol<sup>-1</sup> for L = IMe and PMe<sub>3</sub>, respectively, or allene coordination to give **3**, with an energy

gain of 5.7 and 4.3 kcal mol<sup>-1</sup> for L = IMe and PMe<sub>3</sub>, respectively. Using these different entry points in gold catalysis is another way to address the selective formation of products.

## Experimental Section

All the density functional theory (DFT) calculations were performed using the Gaussian03 package.<sup>[18]</sup> The BP86 GGA functional of Becke and Perdew was used.<sup>[19]</sup> The TZVP triple- $\zeta$  basis set with one polarization function was used for main-group atoms,<sup>[20]</sup> while the relativistic SDD effective core potential in combination with a triple- $\zeta$  basis set was used for the Au atom.<sup>[21]</sup> All geometries were verified by frequency calculations that resulted in 0 and 1 imaginary frequency for intermediates and transition states, respectively. The reported energies include the vibrational gas-phase zero-point energy term. Solvent effects have been obtained through single-point calculations on the gas-phase optimized geometries. The polarizable continuous solvation model IEF-PCM as implemented in the Gaussian03 package has been used.<sup>[22]</sup> CH<sub>2</sub>Cl<sub>2</sub> was chosen as model solvent, with a dielectric constant  $\epsilon = 8.93$ . Standard non-electrostatic terms were also included.

Received: August 16, 2007

Published online: December 14, 2007

**Keywords:** alkynes · allenes · density functional calculations · gold · homogeneous catalysis

- [1] For most recent reviews, see: a) D. J. Gorin, F. D. Toste, *Nature* **2007**, *446*, 395–403; b) A. Fürstner, P. W. Davies, *Angew. Chem.* **2007**, *119*, 3478–3519; *Angew. Chem. Int. Ed.* **2007**, *46*, 3410–3449; c) E. Jiménez-Núñez, A. M. Echavarren, *Chem. Commun.* **2007**, 333–346.
- [2] For a review, see: J. Marco-Contelles, E. Soriano, *Chem. Eur. J.* **2007**, *13*, 1350–1357.
- [3] For Au-mediated 1,2-shift of propargylic esters, see: a) V. Mamane, T. Gress, H. Krause, A. Fürstner, *J. Am. Chem. Soc.* **2004**, *126*, 8654–8655; b) X. Shi, D. J. Gorin, F. D. Toste, *J. Am. Chem. Soc.* **2005**, *127*, 5802–5803; c) M. J. Johansson, D. J. Gorin, S. T. Staben, F. D. Toste, *J. Am. Chem. Soc.* **2005**, *127*, 18002–18003; d) D. J. Gorin, P. Dubé, F. D. Toste, *J. Am. Chem. Soc.* **2006**, *128*, 14480–14481; e) N. Marion, P. de Frémont, G. Lemièrre, E. D. Stevens, L. Fensterbank, M. Malacria, S. P. Nolan, *Chem. Commun.* **2006**, 2048–2050.
- [4] For most recent reports of Au-mediated 1,3-shifts of propargylic esters, see: a) C. H. Oh, A. Kim, W. Park, D. I. Park, N. Kim, *Synlett* **2006**, 2781–2784; b) A. Buzas, F. Gagosz, *J. Am. Chem. Soc.* **2006**, *128*, 12614–12615; c) S. Wang, L. Zhang, *J. Am. Chem. Soc.* **2006**, *128*, 14274–14275; d) H.-S. Yeom, S.-J. Yoon, S. Shin, *Tetrahedron Lett.* **2007**, *48*, 4817–4820; e) G. Lemièrre, V. Gandon, K. Cariou, T. Fukuyama, A.-L. Dhimane, L. Fensterbank, M. Malacria, *Org. Lett.* **2007**, *9*, 2207–2209.
- [5] For alternative reactivities of propargylic esters and related compounds, see: a) L. Zhang, *J. Am. Chem. Soc.* **2005**, *127*, 16804–16805; b) L. Peng, X. Zhang, S. Zhang, J. Wang, *J. Org. Chem.* **2007**, *72*, 1192–1197; c) K. Kato, R. Teraguchi, T. Kusakabe, S. Motodate, S. Yamamura, T. Mochida, H. Akita, *Synlett* **2007**, 63–66; d) N. Marion, P. Carlvqvist, R. Gealageas, P. de Frémont, F. Maseras, S. P. Nolan, *Chem. Eur. J.* **2007**, *13*, 6437–6451.
- [6] Au-mediated 1,3-shift of *allylic* esters is also known, see: a) A. K. Buzas, F. M. Istrate, F. Gagosz, *Org. Lett.* **2007**, *9*, 985–988; b) N. Marion, R. Gealageas, S. P. Nolan, *Org. Lett.* **2007**, *9*, 2653–2656.

- [7] For a review on the reactivity of propargylic esters in the presence of gold catalysts, see: N. Marion, S. P. Nolan, *Angew. Chem.* **2007**, *119*, 2806–2809; *Angew. Chem. Int. Ed.* **2007**, *46*, 2750–2752.
- [8] For a theoretical study of the gold(I)-catalyzed Rautenstrauch rearrangement, see: O. N. Faza, C. S. López, R. Álvarez, A. R. de Lera, *J. Am. Chem. Soc.* **2006**, *128*, 2434–2437.
- [9] For theoretical studies on the reactivity of propargylic acetates in the presence of PtCl<sub>2</sub>, see: a) E. Soriano, P. Ballesteros, J. Marco-Contelles, *Organometallics* **2005**, *24*, 3182–3191; b) E. Soriano, P. Ballesteros, J. Marco-Contelles, *J. Org. Chem.* **2005**, *70*, 9345–9353; c) E. Soriano, P. Ballesteros, J. Marco-Contelles, *J. Org. Chem.* **2007**, *72*, 1443–1448; d) E. Soriano, P. Ballesteros, J. Marco-Contelles, *J. Org. Chem.* **2007**, *72*, 2651–2654.
- [10] For reviews on NHCs in catalysis, see: a) “*N-Heterocyclic Carbenes in Transition Metal Catalysis*”: *Topics in Organometallic Chemistry*, Vol. 28 (Ed.: F. Glorius), Springer, Berlin, **2007**; b) *N-Heterocyclic Carbenes in Synthesis* (Ed.: S. P. Nolan), Wiley-VCH, Weinheim, **2006**.
- [11] For reviews on NHC properties, see: a) S. Díez-González, S. P. Nolan, *Coord. Chem. Rev.* **2007**, *251*, 874–883; b) F. E. Hahn, *Angew. Chem.* **2006**, *118*, 1374–1378; *Angew. Chem. Int. Ed.* **2006**, *45*, 1348–1352; c) L. Cavallo, A. Correa, C. Costabile, H. Jacobsen, *J. Organomet. Chem.* **2005**, *690*, 5407–5413.
- [12] For a review dedicated to NHC–gold(I) complexes, see: I. J. B. Lin, C. S. Vasam, *Can. J. Chem.* **2005**, *83*, 812–825.
- [13] In the present paper we only discuss formation of the *E* isomer around the C1–C2 bond of **1-2** and **2**. Nevertheless, calculations suggest that there is a competitive pathway leading to the formation of the corresponding *Z* isomers.
- [14] The barrier is calculated as the energy difference between the transition states at 2.4 and 0.7 kcal mol<sup>-1</sup> for IMe and PMe<sub>3</sub>, respectively, and intermediate **1-2** at –5.9 and –8.6 kcal mol<sup>-1</sup> for IMe and PMe<sub>3</sub>, respectively. All the other barriers are calculated similarly.
- [15] Issues related to the propargylic ester structure (i.e. propargylic and acetylenic substitutions that have a steric and electronic influence in determining the most favored reaction pathway) are critical but could not be addressed here for reasons of space. They will be examined in a forthcoming full paper.
- [16] B. A. Bhanu Prasad, F. K. Yoshimoto, R. Sarpong, *J. Am. Chem. Soc.* **2005**, *127*, 12468–12469.
- [17] 1,2- and 1,3-OAc shifts in allenyl esters, which can be seen as “retro-migration”, have been observed in the presence of Au, see: a) N. Marion, S. Díez-González, P. de Frémont, A. R. Noble, S. P. Nolan, *Angew. Chem.* **2006**, *118*, 3729–3732; *Angew. Chem. Int. Ed.* **2006**, *45*, 3647–3650; b) T. Schwier, A. W. Sromek, D. M. L. Yap, D. Chernyak, V. Gevorgyan, *J. Am. Chem. Soc.* **2007**, *129*, 9868–9878.
- [18] *Gaussian 03*; Gaussian, Inc.: Pittsburgh, PA, **2003**.
- [19] a) A. Becke, *Phys. Rev. A* **1988**, *38*, 3098–3100; b) J. P. Perdew, *Phys. Rev. B* **1986**, *33*, 8822–8824; c) J. P. Perdew, *Phys. Rev. B* **1986**, *34*, 7406–7406.
- [20] a) A. Schaefer, H. Horn, R. Ahlrichs, *J. Chem. Phys.* **1992**, *97*, 2571–2577; b) A. Schaefer, C. Huber, R. Ahlrichs, *J. Chem. Phys.* **1994**, *100*, 5829–5835.
- [21] a) U. Haeusermann, M. Dolg, H. Stoll, H. Preuss, *Mol. Phys.* **1993**, *78*, 1211–1224; b) W. Kuechle, M. Dolg, H. Stoll, H. Preuss, *J. Chem. Phys.* **1994**, *100*, 7535; c) T. Leininger, A. Nicklass, H. Stoll, M. Dolg, P. Schwerdtfeger, *J. Chem. Phys.* **1996**, *105*, 1052–1059.
- [22] a) M. Cossi, V. Barone, R. Cammi, J. Tomasi, *Chem. Phys. Lett.* **1996**, *255*, 327–335; b) M. T. Cancès, B. Mennucci, J. Tomasi, *J. Chem. Phys.* **1997**, *107*, 3032–3041; c) M. Cossi, V. Barone, B. Mennucci, J. Tomasi, *Chem. Phys. Lett.* **1998**, *286*, 253–260.